Pathological changes in *Fenneropenaeus indicus* experimentally infected with white spot virus and virus morphogenesis

M. Manjusha [a], Resmy Varghese [a], Rosamma Philip [b], A. Mohandas [a], I.S. Bright Singh [a,*]

[a] *National Centre for Aquatic Animal Health, School of Environmental Studies, Cochin University of Science and Technology, Lake Side Campus, Fine Arts Avenue, Kochi 682 016, India*
[b] *Department of Marine Biology, Microbiology and Biochemistry, School of Marine Sciences, Cochin University of Science and Technology, Lake Side Campus, Fine Arts Avenue, Kochi 682 016, India*

ARTICLE INFO

ABSTRACT

To demonstrate pathological changes due to white spot virus infection in *Fenneropenaeus indicus*, a batch of hatchery bred quarantined animals was experimentally infected with the virus. Organs such as gills, foregut, mid-gut, hindgut, nerve, eye, heart, ovary and integument were examined by light and electron microscopy. Histopathological analyses revealed changes hitherto not reported in *F. indicus* such as lesions to the internal folding of gut resulted in syncytial mass sloughed off into lumen, thickening of hepatopancreatic connective tissue with vacuolization of tubules and necrosis of rectal pads in hindgut. Virus replication was seen in the crystalline tract region of the compound eye and eosinophilic granules infiltrated from its base. In the gill arch, dilation and disintegration of median blood vessel was observed. In the nervous tissues, encapsulation and subsequent atrophy of hypertrophied nuclei of the neurosecretory cells were found. Transmission electron microscopy showed viral replication and morphogenesis in cells of infected tissue. *De novo* formed vesicles covered the capsid forming a bilayered envelop opened at one end inside the virogenic stroma. Circular vesicles containing nuclear material was found fused with the envelop. Subsequent thickening of the envelop resulted in the fully formed virus. In this study, a correlation was observed between the stages of viral multiplication and the corresponding pathological changes in the cells during the WSV infection. Accordingly, gill and foregut tissues were found highly infected during the onset of clinical signs itself, and are proposed to be used as the tissues for routine disease diagnosis.

1. Introduction

White spot virus (WSV) causes significant mortalities to several cultured penaeid species. Since its advent in 1992, WSV has greatly affected the shrimp farming industry (Mohan et al., 1997). This pathogen has tropism for organs of mesodermal and ectodermal origin (Wongteerasupaya et al.,1995, 1996; Chang et al., 1996; Flegel et al., 1997; Rajendran et al., 1999; Wang et al., 1999; Vijayan et al., 2003; Yoganandhan et al., 2003). Evidence of histopathological manifestations in the target tissues is one of the criteria used in the diagnosis of WSV infection (Lightner, 1996; Wang et al., 1997). Studies on histopathology, cytopathology, morphogenesis, pathogenesis, pathogenicity and virulence have been reported for both laboratory raised and wild Asian and American shrimp species.

White spot syndrome virus has a broad host range within decapod crustaceans. At least 18 cultured and/or wild penaeid shrimp (Park et al., 1998), eight caridean species (Pramod-Kiran et al., 2002), seven species of lobster (Rajendran et al., 1999), seven species of crayfish (Edgerton, 2004), 38 crab species (Yoganandhan et al., 2003) six non-decapod crustacean species (Hossain et al., 2001), members of the phyla Chaetognata and Rotifera (Yan et al., 2004), polychaete worms (Supak et al., 2005) and some aquatic insect larva (Ramírez-Douriet et al., 2005) have been found susceptible to the virus. Histopathological observations during WSV infection in brief is available regarding shrimp species such as *Penaes monodon* (Durand et al., 1997; Wang et al., 1999, 2000; Mishra and Shekhar, 2005) *Litopenaeus vannamei* and *Marsupenaeus japonicus* (Lu et al., 1997; Lightner et al., 1998; Escobedo-Bonilla et al., 2007; Perez et al., 2005; Pantoja and Lightner, 2003), species of Crabs (Kanchanaphum et al., 1998; Kou et al., 1998) and lobster (Rajendran et al., 1999; Wang et al., 1998; Jiravanichpaisal et al., 2001).

Fenerropenaeus indicus is one of the major commercial species of shrimp aquaculture in Asia endemic to Indian waters and the most wild caught Indian species. It is a good quality, good flavored shrimp, popular with importers in Japan, Western Europe and the USA, Iran, Bangladesh, Malaysia, Thailand, Indonesia and the Philippines. This species is also susceptible to WSV. Despite its

importance in commercial catches as well as in culture, histological investigations on the pathological changes in this species due to WSV have been attempted in very limited extend. The only available data is a briefing by Rajendran et al. (1999) and Rajan et al. (2000) who reported nuclear hypertrophy, cell lysis and tissue degeneration as well as the ultra structural of hypertrophied nucleus. This lack of information prompted to undertake the present study on the histopathological changes due to WSV and viral morphogenesis.

2. Materials and methods

2.1. Source of virus

A brood stock of *P. monodon* obtained from a batch of wild spawners brought from Vishakapatnam, Andhra Pradesh in 1997 by Matsyafed, Government of Kerala, for larval production was the source of the virus. The animals had displayed clinical signs of the disease such as white spots on the inner surface of carapace, reddish pleopods and empty intestine. The presence of WSV was confirmed by transmission electron microscopy (TEM) and diagnostic PCR (Lo et al., 1996).

2.2. Viral inoculum

WSV infected gills (500 mg) from *P. monodon* were macerated in an ice-bathed mortar. A volume of 10 ml of cold PBS (NaCl 8 g, KCl 0.2 g, Na_2HPO_4 1.15 g, KH_2PO_4 0.2 g, double distilled water 1000 ml) was used to make a tissue suspension. The homogenate was centrifuged at 8200g in a refrigerated centrifuge (REMI C.24, India) at 4 °C, and the supernatant was filter-sterilized using a 0.22 μm nitrocellulose membrane (Sartorius India (P) Ltd.). An aliquot (10 μl) was streaked on ZoBell's 2216E agar plates and incubated at 28 ± 1 °C for 72 h to determine the bacterial load of the inoculam.

2.3. Experimental animals

A batch of *F. indicus* from a single broodstock was reared in a hatchery. Juvenile shrimp ($n = 50$, mean body weight (MBW) = 3 ± 1) were used for virus amplification and subsequently to perform the experiments. Prior to the experimental infections, shrimps were subjected to a formaline stress test for one hour in seawater (20 g/l) containing 100 ppm formaline with adequate aeration. They were subsequently observed for three days for the manifestation of diseases and mortality. Animals were confirmed to be WSV negative by PCR analysis.

2.4. Experimental infection

An aliquot of 0.01 ml filtrate was injected at the dorsal side of the abdomen of *F. indicus* between telson spine and 6th abdominal segment using 1 ml tuberculin syringe. Animals ($n = 25$) were intramuscularly inoculated (with the WSV inoculum). Groups of Five animals were placed in a fiber-glass tank ($40 \times 25 \times 10$ cm) with sea water having 20 g/l salinity at ambient temperature (28 ± 1 °C) with continuous aeration. Shrimps were fed *ad libitum* with a commercial feed ('Grower' from Higashimaru, India) containing 40% protein. Fresh filtered seawater (about 7 l) with the same salinity and temperature was daily replaced. Animals were monitored for clinical signs of infection such as feeding cessation, lethargy and mortality. Moribund shrimps were fixed for histopathology and electron microscopy as described below. A group of uninfected animals ($n = 10$; two from each set) was used as a control and processed in the same way as the experimental shrimps.

2.5. Histopathology

Moribund as well as control animals having MBW 3 ± 1 g were fixed by injecting 1–3 ml (depending on size) Davidson's fluid on the dorsal side of 6th segment. Immediately after the injection, cuticle was split sagittally and the whole animal immersed in 15 ml Davidson's fluid per animal in screw capped tubes for 24 h. Subsequently, the animals were dissected, and gills, heart, nerve cord, stomach, foregut, mid-gut, hindgut, hepatopancreas, eye, integument and ovary were transferred to 70% ethyl alcohol, processed for histopathology and double stained with haematoxylin and eosin (Bell and Lightner, 1988), and examined under light microscope (Nikon Type 104, Japan).

2.6. Electron microscopy

For electron microscopy gill, foregut, heart, hepatopancreatic connective tissue, hindgut and nerve tissues from WSV infected *F. indicus* as well as those of healthy control animals were removed, minced into 1 mm sized pieces and fixed in 2.5% glutaraldehyde in PBS (1 M, pH 7.4) for 24 h at 4 °C and post fixed in 2% osmium tetroxide in PBS (1 M, pH 7.4) for 2 h at 4 °C. After dehydration through an ascending series of acetone, the tissue pieces were embedded in epoxy resin (Electron Microscopy Sciences, USA). Ultra thin (0.5 μl) sectioned, stained with uranyl acetate and lead citrate, and examined under transmission electron microscope (Philips, CM-10). Based on the ultrastructure of the infected nuclei viral morphogenesis was investigated.

3. Results and discussion

3.1. Histopathology

PCR negative healthy animals which survived formaline stress test were used for the experiment. Presence of WSV in the source tissue as well as the inoculum was confirmed by TEM (Fig. 1a) and diagnostic PCR (Fig. 1b). The viral inoculum showed zero CFU/ml in ZoBell's 2216E agar plate confirming the absence of bacteria in the preparation. Injected animals showed erratic swimming and cessation of feeding after 30–48 h, and with out waiting for mortality they were fixed and processed as described above.
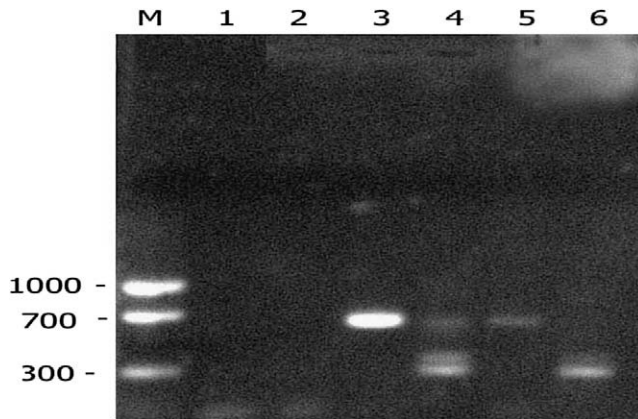
3.2. Digestive system

3.2.1. Foregut
The ventral median channel, ventro lateral folds, and the dorsal grooves, dorsal median folds and intra lateral cardiac plate of the
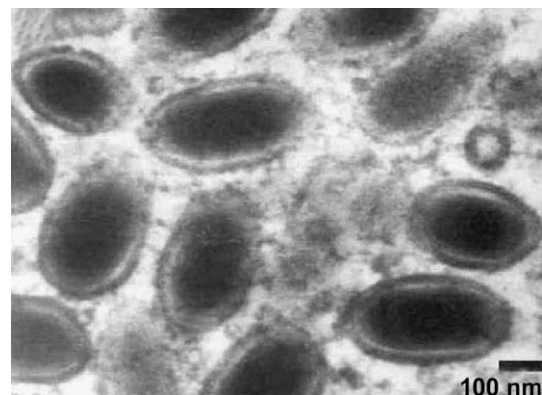
Fig. 1a. TEM of hypertrophied nucleus of gill tissue of *F. indicus* stained with uranyl acetate and lead citrate. Characteristic rod-shaped virions of WSV are seen.

Fig. 1b. Agarose gel with 650 and 300 bp amplified fragments of WSV genome extracted from gill tissue of *Penaeus monodon*. M: Molecular weight marker (1000, 700, and 300 bp); Lane 1: 1 step PCR negative control; lane 2: 2 step PCR negative control; lane 3: 1 step PCR positive control; lane 4: 2 step PCR positive control; lane 5: 1 step PCR product of WSV genome from *F. indicus* infected with WSV; lane 6: 2 step PCR product of WSV from *F. indicus* infected with WSV.

foregut were markedly degenerated and disintegrated in WSV infected *F. indicus*. The foregut cuticular epithelium was one of the target tissues in which the viral infection could be demonstrated as hypertrophied nuclei (Sudha et al., 1998; Mohan et al., 1998). In *L. vannamei*, foregut epithelium is found to be the primary site of replication post infection (Escobedo-Bonilla et al., 2007). The underlying muscular layer of the foregut showed multifocal necrosis. Vacant area formation due to complete disintegration of cells was also reported earlier (Karunasagar et al., 1997; Wongteerasupaya et al., 1995; Chang et al., 1996). This observation was supported by the ultrastructure of the infected nuclei loaded with bunches of fully assembled virions towards the margin of nucleus (289–362 nm long and 144–217 nm wide) suggesting final stage of infection (Fig. 2a). Histopathology and electron microscopy showed the severity of the viral infection in the foregut. Therefore, the lack of feeding behavior is the result of WSV infection and the damage to tissues of the digestive system.

3.2.2. Stomach

The stomach wall of infected specimens was observed disintegrated and detached from the outer cuticular lining coupled with lysis and disintegration of the epithelial layer. The detached stomach wall had transformed into a syncytium. Similar observation of cell lysis and sloughing off of the inner epithelium were correlated
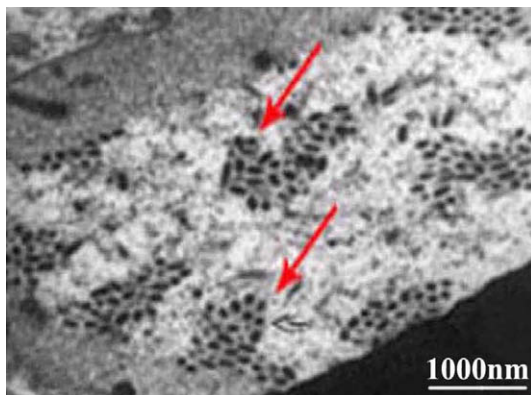
with cessation of feed intake in *P. monodon* as described by Chang et al. (1996). Hypertrophied nuclei were not seen as there was total lysis and sloughing off of inner epithelial layer. This indicated advanced stage of WSV infection at the time of fixation of the tissue.
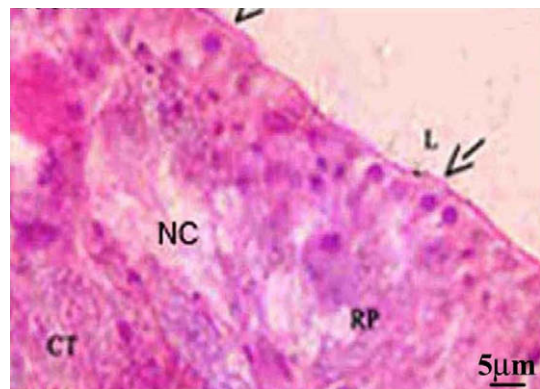
3.2.3. Hepatopancreas

Under TEM, viral particles in the process of multiplication could be seen in nuclei of the connective tissue but not in hepatopancreocytes. Therefore, it could be reasonably inferred that collapse of the supportive connective tissue was responsible for the profound pathological changes of hepatopancreatic tubules; nevertheless, they themselves were not susceptible to the virus. This result agrees with the studies done in *P. monodon* (Chang et al., 1996; Wang et al., 1999) and *L. vannamei* (Escobedo-Bonilla et al., 2007) which revealed virus replication in the myoepithelial cells of the hepatopancreatic sheath and cells of the connective tissues but not in the hepatopancreatic tubular epithelial cells.

3.2.4. Mid-gut

Thin columnar epithelial cells which formed the epithelial lining of the mid-gut with small oval nuclei had undergone extensive atrophy and were sloughed off to the lumen. The circular and longitudinal muscle layers situated beneath the epithelial layer showed extensive multi focal necrosis. The ultra structure of cells showed intranuclear virus replication. Very narrow electron lucent stoma surrounding the chromatin (Fig. 2b) and a few vesicular
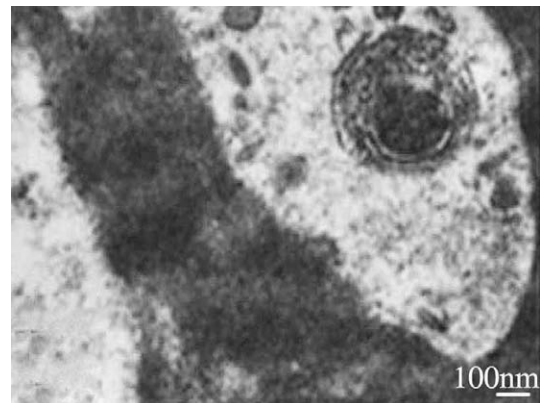
Fig. 2b. TEM of mid-gut nucleus of the WSV infected *F. indicus* having narrow electron lucent stroma with surrounding chromatin and vesicular structures in the less electron dense zone.

Fig. 2a. TEM of the foregut endothelial cell nucleus having bunches of WSV particles inside virogenic stroma and a peripheral ring zone. Arrows indicate viral particles.

Fig. 2c. Enlarged view of rectal pad (RP) of infected *F. indicus* hindgut. Arrow points to hypertrophied nuclei of endothelial cells. The underlying connective tissue (CT) shows necrosis (NC).
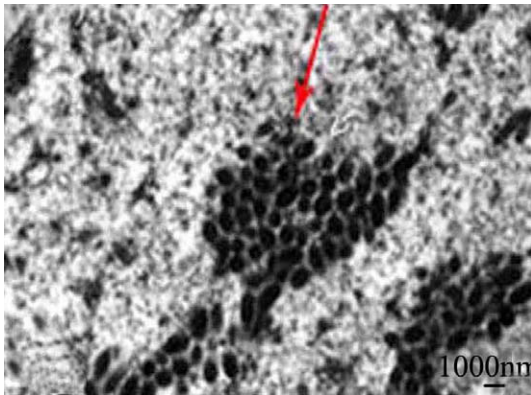
Fig. 2d. TEM presenting bunches of fully formed virions in the hindgut endothelial lining (arrow) towards margin with thin marginal zone and vacant internal virogenic stroma indicating later stages of WSV infection.

Fig. 2f. Transmission electron micrograph of the infected gill nucleus containing bunches of fully formed virions arranged in Paracrystalline array (arrow) towards periphery of the nucleus with large virogenic stroma and thin outer ring zone indicating later stage of WSV infection.

structures in the less electron dense zone were observed. In cells of mid-gut epithelium, virus replication was not found. These pathological changes suggested that these cells were not affected by WSV infection. This observation agrees with the findings of Lo et al. (1997) where in the nuclei were not so obviously hypertrophied and remained close to normal sizes. Also WSV was only able to infect the connective tissue of mid-gut some time after the infection of tissues in the stomach wall (Chang et al., 1996). Another study on *M. japonicus* inoculated per os described epithelial cells of the mid-gut trunk as the primary WSV replication sites (Di Leonardo et al., 2005).
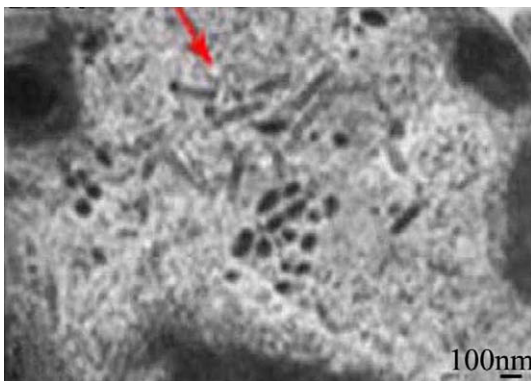
3.2.5. Hindgut

The epithelial lining of the hindgut called rectal pads with the lumen in between (Fig. 2c) showed nuclear hypertrophy, degeneration and necrosis of the underlying connective tissue in the infected animals. This organ clearly supported active viral replication. Ultrastructure showed nuclei with bunches of fully formed virions towards the margin with very thin marginal zone and vacant internal virogenic stroma indicating later stages of viral replication. Virions ranged from 347 nm long to 173 nm wide (Fig. 2d).
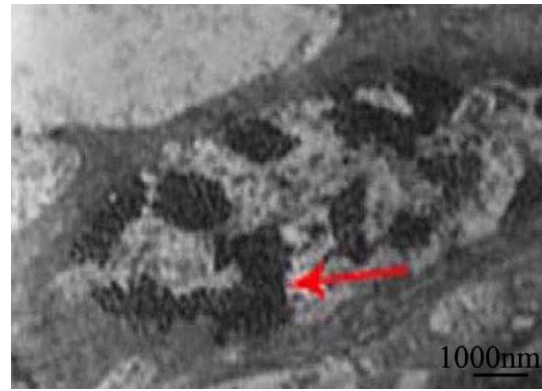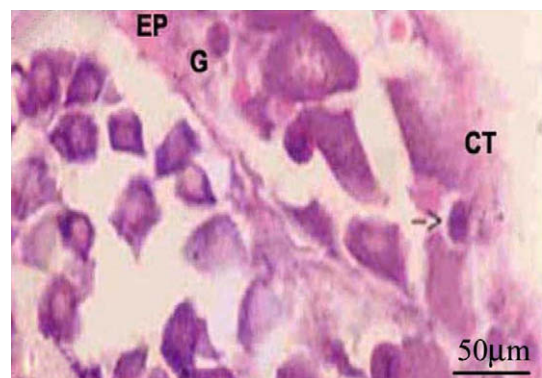
3.3. Nervous system

3.3.1. Nerve

The endothelial lining of the blood sinus inside the nerve sheath had lost its integrity. The neurosecretory cells were with hypertro-

phied nuclei and eosinophilic inclusions, and in a few instances with haemocytic encapsulation and subsequent atrophy. The haemocytes were deeply stained and dense in appearance. The eosinophilic stage of hypertrophied nuclei was seen sporadically in the tissue. Under TEM hypertrophied nuclei were with virions at different stages of formation (Fig. 2e). This included envelop, empty capsid, partially filled capsid, probable point of entry of nuclear material to capsid and fully formed virions. The nucleocapsid had a length of 318–463 nm and a width of 46–86 nm. Fully formed virions recorded a length of 240–318 nm and 115–144 nm width. Virus replication at different stages of morphogenesis was observed in this tissue even when animals were moribund. Previous studies showed that connective tissue of the nervous system were alone infected by WSV (Karunasagar et al., 1997; Sudha et al., 1998; Wang et al., 1999; Escobedo-Bonilla et al., 2007). It is therefore concluded that both neurosecretory and connective tissue of the nervous system are equally susceptible to WSV infection.

3.4. Eye

The layer of retinular cell nuclei of the eyes showed lysis and had lost its integrity compared to the eye of healthy shrimp. The eye of WSV infected shrimp showed tissue damage in the crystalline tract region and the nuclei of the crystalline tract cells were hypertrophied with necrosis of the tissue forming undifferentiated mass followed by spontaneous infiltration of oesinophilic granules from the base of the crystalline cone. Origin of these granules could not be identified for which more research is needed. Despite that

Fig. 2e. TEM of nucleus of nerve tissue of WSV infected *F. indicus* presenting different stages of virus morphogenesis (arrow) in the virogenic stroma with marginated chromatin.

Fig. 2g. Ovarian tissue of infected *F. indicus* presenting necrotic connective tissue (CT), germinal layer (G) and epithelium (EP). Arrows point to hypertrophied nuclei.

no hypertrophied cells could be detected in the lamina ganglionaris region, necrosis was observed.

3.5. Cardiovascular system

3.5.1. Heart

Hypertrophied nuclei could not be demonstrated in heart tissues. However, a generalized vacuolization of the tissue as a whole and constriction of muscle bundles along with increased infiltration of blood cells in between the muscle bundles and oedema in the heart wall were seen. The nuclei remained close to normal and virus replication was poor in its magnitude as characterized by a broad ring zone and a smaller virogenic stroma, and was found disorganized with fewer virions whose sizes ranged from 260 to 347 nm in length and from 144 to 160 nm in width.

3.6. Respiratory system

3.6.1. Gills

The dendrobranchiate gill consisting of a median gill axis and the gill filament showed massive disintegration and vacuolization in infected shrimps. The median blood vessel which traversed longitudinally along the septa of the main axis had dilated and laterally ruptured in the infected shrimp. The gill filaments in apparently healthy animals contained numerous lacunae occluded by hemocytes. During infection they showed massive disintegration and generalized vacuolization and the nuclei of the epithelial cells were hypertrophied. TEM revealed bunches of fully formed virions in paracrystalline array towards the margin of the hypertrophied nuclei showing the later stage of viral replication. The virions ranged from 267 to 317 nm long and from 105 to 158 nm wide (Fig. 2f). In *L. vennamei* higher proportion of hypertrophied cells showed hydropic degeneration, and some areas of focal necrosis after 48 h post infection, and gill epithelium was found to be the primary site for viral replication (Escobedo-Bonilla et al., 2007). Normally when the animals get infected they come to the surface of water and move towards the periphery of the pond apparently to get more oxygen, a behavioral trait considered as an outward manifestation of the impairment of breathing capacity.

3.7. Reproductive system

3.7.1. Ovary

All three layers of the ovarian wall, outer epithelial layer, a comparatively thicker connective tissue, and the innermost germinal layer showed necrosis (Fig. 2g). Hypertrophied nuclei were not seen in the developing oocytes but the nuclei of the connective tissue were found enlarged and hypertrophied. This is similar to the earlier observations that immature gonads of female or male juveniles showed WSV infected cells in the connective tissues only (Escobedo-Bonilla et al., 2007). Previous studies employing fluorescent *in situ* hybridization with *P. monodon* brooders (Lo et al., 1997) or with *P. monodon* of undetermined age (Chang et al., 1998) have shown that the connective tissues and muscle sheaths around the ovary or testes/spermatophore are susceptible to WSV infection. Earlier studies indicated that oocytes did not show any sign of viral invasion (Sudha et al., 1998). Therefore, it could be reasonably believed that the release of viral particles from ovarian connective tissue along with oocytes during spawning and the subsequent infection of the latter might be the mode of vertical transmission (Escobedo-Bonilla et al., 2007). In the ovary of *P. monodon* brooders, WSV was detected in follicle cells and oogonia. A few developing oocytes were WSV positive. In testes, no reproductive cells were found infected with WSV (Lo et al., 1997). However, a clear evidence of infection in oocytes, with the presence of dense baso-

philic intranuclear inclusions could be seen; severely infected oocytes were unable to develop further and probably die before maturation (Wang et al., 1999).

3.8. Skeletal system

3.8.1. Integument

The outer exocuticle and the underlying procuticular layers of the integument had lost their integrity after WSV infection. The carapace at the time of fixation had shown characteristic white spots. The integument showed cells with hypertrophied nuclei and massive necrosis. In several epizootics of WSV infection, moderate softening of the exoskeleton has been reported. As a rule the underlying epithelial layer plays a vital role in maintaining the structural integrity of the exo and pro cuticle.

3.9. Morphogenesis

Viral morphogenesis was investigated using *F. indicus* as animal model as presented in Figs. 3a–3g. In all ultrathin sections observed, peripheral margination of chromatin and formation of middle electron lucent central virogenic stroma could be demonstrated as the prelude of viral replication. (Durand et al., 1997; Wang et al., 1999, 2000). A prominent structure was the elongated empty capsid with a trilaminar outer envelop. Some of the capsids were closed at one end while others had both the ends open. Empty vesicles were seen in the virogenic stoma suggesting the formation of new envelops. The capsid became progressively dense with an electron dense nuclear material. Viral multiplication took place in the virogenic stroma in locci where they were arranged in paracrystalline array during assembly. Based on the evidence obtained in the present investigation the sequence in viral morphogenesis initiates with the *de novo* synthesis of virus nuclear material, capsid and envelop within the virogenic stroma of the nucleus. Later, they migrate to various loci of virogenic stroma for virus assembly. The trilaminar envelop with one open end slides over the capsid forming an outer covering. Meanwhile, the virus nuclear materials get surrounded by vesicles which fuse with the already enveloped capsid releasing the viral nuclear material into the core of the capsid. Once the capsid gets filled, the vesicular structure fuses with the envelop to form fully assembled virions. While the virus assembly takes place they assume a paracrystalline structure which later gets loosened facilitating migration of the virions towards the base of the nuclear membrane within the narrowed marginated chromatin. The nuclear membranes lyse releasing the
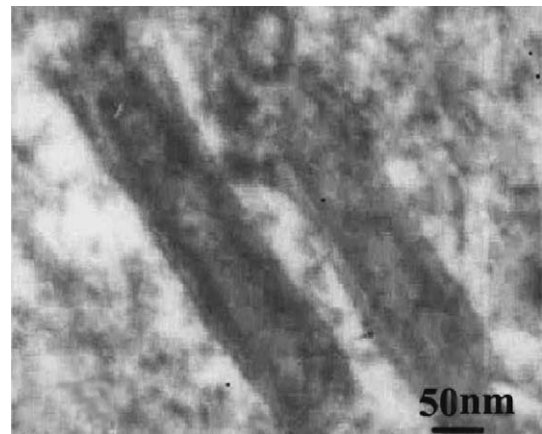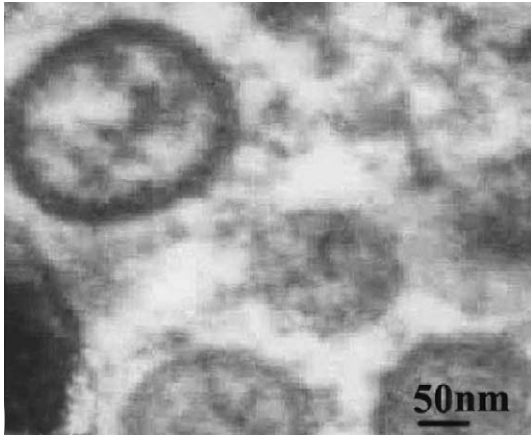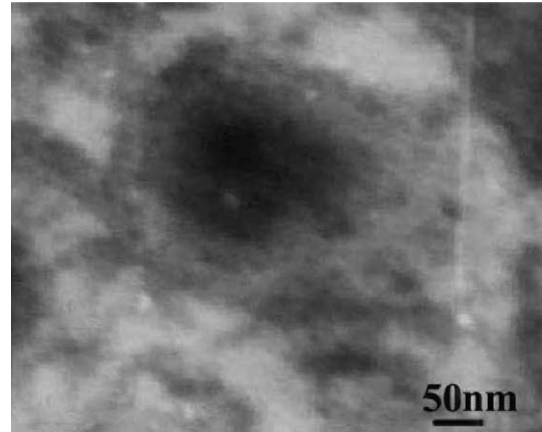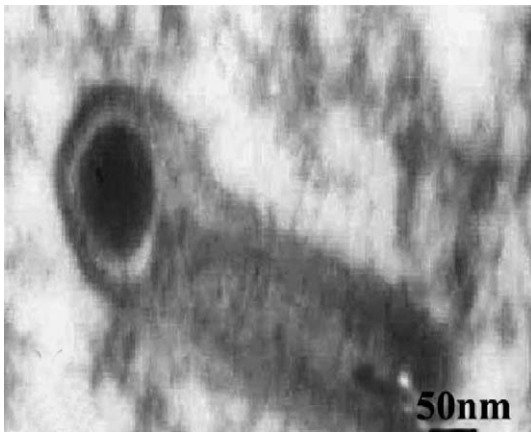

**Fig. 3a.** TEM of elongated empty capsid with trilaminar outer envelop.

Fig. 3b. TEM of cross section of tubular structures with trilaminar layer characteristic of the viral envelop.
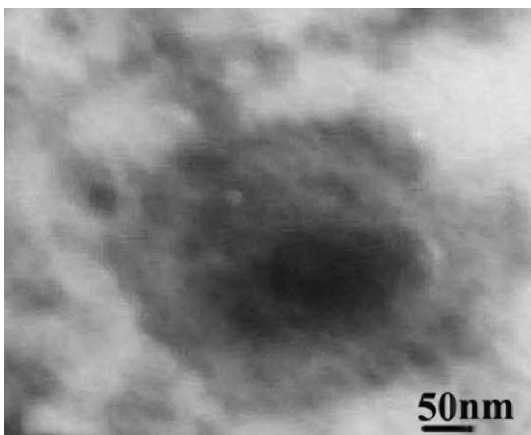

Fig. 3e. TEM of different stages in the progressive densification of the envelop capsid.
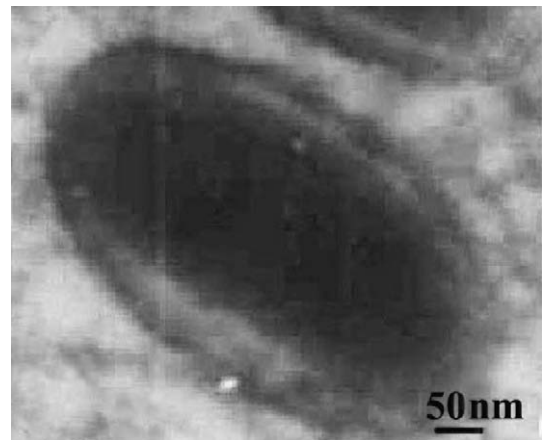

Fig. 3c. TEM of fusion of nuclear material borne by a trilaminar vesicle with capsid just before its delivery into the capsid core.
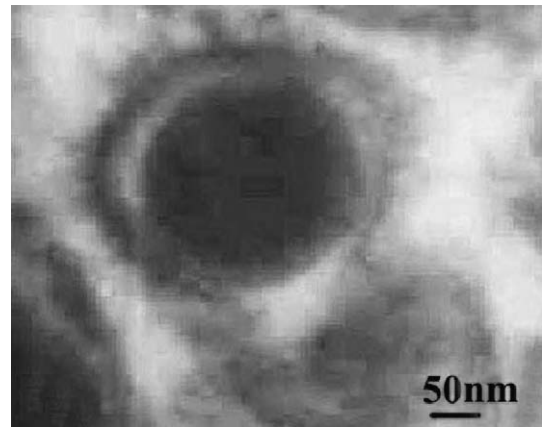
Fig. 3f. TEM of different stages in the progressive densification of the envelop capsid.

Fig. 3d. TEM of different stages in the progressive densification of the envelop capsid.

Fig. 3g. TEM of fully assembled WSV.

virions to cytoplasm from where the virus gets released when the animal dies and cells decay.

The observations are similar to that of *P. monodon* (Durand et al., 1997; Wang et al., 1999; Tsai et al., 2006) except the formation of a tail like extension by the envelop. We could not find such an elongation of envelop in any of our preparation, instead fusion of trilaminar circular vesicles containing nuclear materials with the enveloped capsid was observed. And there was no evidence of the trilaminar envelops being derived from the nuclear membrane. Instead, it appeared that the lipid envelop was synthesized within the nucleus by transporting the precursors from cytoplasm across the nuclear membrane.

The present study describes in detail the histological changes that occur in various tissues of *F. indicus* during WSV infection. This

include the presence of hypertrophied nuclei, tissue disintegration and necrosis, hemocytic infiltration, vacuolization and edema as reported by the earlier workers (Escobedo-Bonilla et al., 2008) However, certain pathological changes which are hitherto not reported are listed here that include damages to the internal folding of the gut, formation of syncytial mass in the stomach endothelium and its sloughing off into the lumen, thickening of the hepatopancreatic connective tissue with complete vacuolization of the tubules, necrosis of the rectal pads in hindgut, viral multiplication in the crystalline tract region of the eye ball and infiltration of eosinophilic granules from the base of crystalline cone, dilation and disintegration of median blood vessel of the gill arch, encapsulation and subsequent atrophy of hypertrophied nuclei of the neurosecretory cells by the darkly staining hemocytes in nerve tissues. Ultra structural observation of these tissues revealed various stages of WSV replication in the nuclei depending upon the degree of infection. Thus forgut, gill and hindgut nuclei had wider virogenic stroma, narrow ring zone and fully formed enveloped virus indicating higher infection stage, while nuclei of nerve, heart, and mid-gut showed smaller virogenic stroma, a broader ring zone and few virus particles indicating initial stages of viral infections. Hepatopancreatic connective tissue nuclei had fully formed virus packed in it but not so hypertrophied. Corresponding changes were observed in the cytoplasm according to the stages of infection. There was greater degree of correlation between the two modes of investigations in depicting its severity. Thus by TEM and histology it was demonstrated that gill, foregut and hindgut were the most severely infected tissues having large virogenic stroma, narrow ring zone and fully formed virus inside the nuclei with extensive necrosis and disintegration of cytoplasm which could be attributed to the cessation of feeding and erratic swimming, to the surface. Conversely, small numbers of WSV infected cells were found in the heart, nerve cord and eye tissues. By a similar study using immunohistochemistry, foregut, gill, antennal gland and integument were found to be the primary site of viral replication in *L. vannamei*. Epithelial cells in these organs were increasingly damaged as WSV infection progressed, which most probably led to dysfunction of these organs and death. (Escobedo-Bonilla et al., 2007). By this study gill and foregut epithelia were demonstrated as the primary target of WSV infection and could be utilized for the routine WSV disease diagnosis.

Acknowledgments

References

Bell, T.A., Lightner, D.V., 1988. A Handbook of Normal Penaeid Prawn Histology. World Aquaculture Society.

Chang, P.S., Lo, C.F., Wang, Y.C., Kou, G.H., 1996. Identification of white spot syndrome associated baculovirus (WSBV) target organs in the prawn *P. monodon*, by in situ hybridization. Dis. Aquat.Org. 27, 131–139.

Chang, P.S., Chen, H.C., Wang, Y.C., 1998. Detection of white spot syndrome associated baculovirus in experimentally infected wild shrimp, crabs and lobsters by in situ hybridization. Aquaculture 164, 233–242.

Di Leonardo, V., Bonnichon, V., Roch, P., Parrinello, N., Bonami, J.R., 2005. Comparative WSSV infection routes in the shrimp genera *Marsupenaeus* and *Palaemon*. J. Fish Dis. 28, 565–569.

Durand, S., Lightner, D.V., Redman, R.M., Bonami, J.R., 1997. Ultrastructure and morphogenesis of white spot syndrome baculovirus (WSSV). Dis. Aquat. Org. 29, 205–211.

Edgerton, B.F., 2004. Susceptibility of the Australian freshwater crayfish Cherax destructor albidus to white spot syndrome virus (WSSV). Dis. Aquat. Org. 59, 187–193.

Escobedo-Bonilla, C.M., Alday-Sanz, V., Wille, M., Sorgeloos, P., Pensaert, M.B., Nauwynck, H.J., 2008. A review on the morphology, molecular characterization, morphogenesis and pathogenesis of white spot syndrome virus. J. Fish Dis. 31, 1–18.

Escobedo-Bonilla, C.M., Wille, M., Alday-Sanz, V., Sorgeloos, P., Pensaert, M.B., Nauwynck, H.J., 2007. Pathogenesis of a Thai strain of white spot syndrome virus (WSSV) in SPF *Litopenaeus vannamei*. Dis. Aquat. Org. 74, 85–94.

Flegel, T.W., Boonyaratpalin, S., Withyachumnarnkal, B., 1997. Current status of research on yellow head virus and white spot virus in Thailand. In: Third Symposium on diseases in Asian Aquaculture, Bangkok, Thailand, 29 January–February 1996.

Hossain, S., Chakraborty, A., Joseph, B., Otta, S.K., Karunasagar, I., Karunasagar, I., 2001. Detection of new hosts for white spot syndrome virus of shrimp using nested polymerase chain reaction. Aquaculture 198, 1–11.

Jiravanichpaisal, P., Bangyeekhum, E., Söderhäll, K, L. Söderhäll., 2001. Experimental infection of white spot syndrome virus in freshwater crayfish *Pacifastacus leniusculus*. Dis. Aquat. Org. 47, 151–157.

Kanchanaphum, P., Wongteerasupaya, C., Sitidilokratana, N., Boonsaeng, V., Panyim, S., Tassanakajon, A., Withyachumnarnkul, B., Flegel, T.W., 1998. Experimental transmission of white spot syndrome virus (WSSV) from crabs to shrimp *Penaeus monodon*. Dis. Aquat. Org. 34, 1–7.

Karunasagar, I., Otta, S.K., Karunasagar, I., 1997. Histopathological and bacteriological study of white Spot syndrome of *Penaeus monodon* along the West Coast of India. Aquaculture 153, 9–13.

Kou, G.H., Peng, S.E., Chiu, Y.L., Lo, C.F., 1998. Tissue distribution of white spot syndrome virus (WSSV) in shrimp and crabs. In: Flegel, T.W. (Ed.), Advances in Shrimp Biotechnology. National Center for Genetic Engineering and Biotechnology, Bangkok, pp. 267–271.

Lightner, D.V., 1996. A Handbook of Pathology and Diagnostic Procedures for Diseases of Penaeid Shrimp. World Aquaculture Society.

Lightner, D.V., Hasson, K.W., White, B.L., Redman, R.M., 1998. Experimental infection of western hemisphere penaeid shrimp with Asian white spot syndrome virus and Asian yellow head virus. J. Aquat. Anim. Health 10, 271–281.

Lo, C.F., Ching, H.H., Chau, H.C., Kuan, F.L., Ya, L.C., Pei, Y.Y., Shao, E.P., Hui, C.H., Hwei, C.L., Chen, F.C., Mao, S.S., Chung, H.W., Guang, H.K., 1997. Detection and tissue tropism of white spot syndrome baculovirus (WSBV) in captured brooders of *Penaeus monodon* with a special emphasis on reproductive organs. Dis. Aquat. Org. 30, 53–72.

Lo, C.F., Jiann, H.L., Ching, H.H., Chau, H.C., Shao, E.P., You, T.C., Chih, M.C., Pei, Y.Y., Chang, J.H., Hsin, Y.C., Chung, H.W., Guang, H.K., 1996. Detection of baculovirus associated with white spot syndrome (WSBV) in penaeid shrimps using polymerase chain reaction. Dis. Aquat. Org. 25, 133–141.

Lu, Y., Tapay, L.M., Loh, P.C., Gose, R.B., Brock, J.A., 1997. The pathogenicity of a baculo-like virus isolated from diseased penaeid shrimp obtained from China for cultured penaeid species in Hawaii. Aquat. Int. 5, 277–282.

Mishra, S.S., Shekhar, M.S., 2005. White spot syndrome virus isolates of tiger shrimp *Penaeus monodon* (Fabricious) in India are similar to exotic isolates as revealed by polymerase chain reaction and electron microscopy. Indian J. Exp. Biol. 43, 654–661.

Mohan, C.V., Shankar, K.M., Kulkarni, S., Sudha, P.M., 1998. Histopathology of cultured shrimps showing gross signs of yellow head syndrome and white spot syndrome during 1994, Indian epizootics. Dis. Aquat. Org. 34, 9–12.

Mohan, C.V., Sudha, P.M., Shanker, K.M., Hegde, A., 1997. Vertical transmission of white spot baculovirus in shrimp – a possibility. Curr. Sci. 73, 109–110.

Park, J.H., Lee, Y.S., Lee, S., Lee, Y., 1998. An infectious viral disease of penaeid shrimp newly found in Korea. Dis. Aquat. Org. 34, 71–75.

Pantoja, C, R., Lightner, D.V., 2003. Similarity between the histopathology of white spot syndrome virus and yellow head syndrome virus and its relevance to diagnosis of YHV disease in the Americas. Aquaculture 218, 47–54.

Perez, F., Volckaert, F.A.M., Calderon, J., 2005. Pathogenicity of white spot syndrome virus on post larvae and juveniles of *Penaeus* (*Litopenaeus*) *vannamei*. Aquaculture 205, 586–591.

Pramod-Kiran, R., Rajendran, K., Jung, S., Oh, M., 2002. Experimental susceptibility of different life-stages of the giant freshwater prawn *Macrobrachium rosenbergii* (de Man), to white spot syndrome virus (WSSV). J. Fish Dis. 25, 201–207.

Rajan, P.R., Ramasamy, P., Purushothaman, V., Brennan, G.P., 2000. White spot baculovirus syndrome in the Indian shrimp *Penaeus monodon* and *P. indicus*. Aquaculture 184, 31–44.

Rajendran, K.V., Vijayan, K.K., Santiago, T.C., Krol, R.M., 1999. Experimental host range and histopathology of white spot syndrome virus (WSSV) infection in shrimp, prawns, crabs and lobsters from India. J. Fish Dis. 22, 183–191.

Ramírez-Douriet, C., De Silva-Da´vila, R., Me´ndez-Lozano, J., Escobedo-Urias, D., Leyva-Arana, I., López-Meyer, M., 2005. White spot syndrome virus detection in zooplankton of coastal lagoons and shrimp commercial ponds in Sinaloa, Mexico. In: 135 Annual Meeting of the American Fisheries Society, Anchorage, Alaska.

Sudha, P.M., Mohan, C.V., Shankar, K.M., Hegde, A., 1998. Relationship between white spot syndrome virus infection and clinical manifestation in Indian cultured penaeid shrimp. Aquaculture 167, 95–101.

Supak, L.S., Boonnat, A., Poltana, P., Kanchanaphum, P., Gangnonngiw, W., Nash, G., Withyachumnarnkul, B., 2005. Infectivity of white spot syndrome virus (WSSV) to the polychaete *Pereneis nuntia* and a possibility of WSSV transmission from the polychaete to the black tiger shrimp *Penaeus monodon*. In: Walker, P.J., Lester, R., Bondad-Reantaso, M.G. (Eds.), Diseases in Asian Aquaculture V. Fish Health Section. Asian Fisheries Society, Manila, Philippines, pp. 353–361.

Tsai, J.M., Wang, H.C., Leu, J.H., Wang, A.H.J., Zhuang, Y., Walker, P.J., Kou, G.H., Lo, C.F., 2006. Identification of the nucleocapsid, tegument and envelop proteins of the shrimp white spot syndrome virus virion. J. Virol. 80, 3021–3029.

Vijayan, K.K., Balasubramanian, C.P., Jithendran, K.P., Alavandi, S.V., Santiago, T.C., 2003. Histopathology of Y-organ in Indian white shrimp *Fenneropenaeus indicus*, experimentally infected with white spot syndrome virus. Aquaculture 221, 97–106.

Wang, Y.C., Lo, C.F., Chang, P.S., Kou, G.H., 1998. Experimental infection of white spot baculovirus in some cultured and wild decapods in Taiwan. Aquaculture 164, 221–231.

Wang, C.H., Yang, H.N., Tang, C.Y., Lu, C.H., Kou, G.H., Lo, C.F., 2000. Ultra structure of white spot syndrome virus development in primary lymphoid organ cell cultures. Dis. Aquat. Org. 41, 91–104.

Wang, Y.G., Hassan, M.D., Shariff, M., Zamri, S.M., Chen, X., 1999. Histopathology and cytopathology of white spot syndrome virus (WSSV) in cultured *Penaeus monodon* from peninsular Malaysia with emphasis on pathogenesis and the mechanism of white spot formation. Dis. Aquat. Org. 39, 1–11.

Wang, C.S., Tang, K.F.J., Kou, G.H., Chen, S.N., 1997. Light and electron microscopic evidence of white spot disease in the giant tiger shrimp, Penaeus monodon, Penaeus japonicus. J. Fish Dis. 20, 323–331.

Wongteerasupaya, C., Panyim, S., Wongwisansri, S., Pratanpipat, P., Boonsirm, V.G., Nash, L., Withyachumnarnkul, B., Flegel, T.W., 1996. DNA fragment of *Penaeus monodon* baculovirus PmNOB II gives positive *in situ* hybridization with white spot viral infections in six penaeid shrimp species. Aquaculture 143, 23–32.

Wongteerasupaya, C., Vickers, J.E., Sriurairatna, S., Nash, G.L., Akarajamorn, A., Boonsaeng, V., Panyim, S., Tassanakajon, A., Withyachumnarakul, B., Flegel, T.W., 1995. A non-occluded systemic baculovirus that occurs in cells of ectodermal and mesodermal origin and causes high mortality in the black tiger prawn *Penaeus monodon*. Dis. Aquat.Org. 21, 69–77.

Yan, D.C., Dong, S.L., Huang, J., Yu, X.M., Feng, M.Y., 2004. White spot syndrome virus (WSSV) detected by PCR in rotifers and rotifer resting eggs from shrimp pond sediments. Dis. Aquat. Org. 59, 69–73.

Yoganandhan, K., Sathish, S., Murugan, V., Narayanan, R.B., Sahul Hameed, A.S., 2003. Screening the organs for early detection of white spot syndrome virus in *Penaeus indicus* by histopathology and PCR techniques. Aquaculture 215, 21–29.